IOP Conf. Series: Materials Science and Engineering **258** (2017) 012001 doi:10.1088/1757-899X/258/1/012001

Correlation between the dielectric and the mechanical behavior of cellulose nanocomposites extracted from the rachis of the date palm tree

A Ladhar[1], M Arous[1], H Kaddami[2], Z Ayadi[3*], A Kallel[1*]

[1] LaMaCoP, Faculty of Sciences of Sfax, University of Sfax, BP 3018 Sfax, Tunisia
[2] LCBM, Faculty of Sciences and Technologies, Cadi-Ayyad University, 40000 Marrakech, Morocco
[3] EEIGM, Equipe PMP-304, Nancy, France

*zoubir.ayadi@univ-lorraine.fr; ali.kallel@fss.rnu.tn

Abstract. In the present study, the dielectric and mechanical properties of natural rubber (NR) based nanocomposites are investigated. Cellulose nanofillers are used in two forms as reinforcing phase: nanofibrillated cellulose (NFC) and cellulose nanocrystals (CNC). In the dielectric study, different relaxation phenomena are detected: the α dipolar relaxation, the lignin and hemicelluloses relaxation, the water dipoles relaxation, the interfacial polarization and the ionic conduction. For the interfacial polarization, the dielectric strength $\Delta\varepsilon$ showed lower values for NFC-filled nanocomposites than CNC-filled samples. It was explained with higher interactions between induced dipoles and lower mobility, assuring a better adhesion between the NR and the NFC. Moreover, in tensile tests, the elastic modulus increases with filling indicating the reinforcement effect of nanofillers. In addition, the NR-NFC nanocomposites display the highest tensile modulus. This result shows the higher compatibility of NFC with the NR matrix, and the ensuing higher filler/matrix adhesion. In dynamic mechanical analysis (DMA), a significant reinforcing effect of NFC was shown. This effect is manifested with the high storage modulus E', suggesting that the interactions between the NR matrix and the NFC fibers were stronger.

1. Introduction

Nowadays, two major problems are encountered in the polymer industry: (*i*) the problem of pollution due to the use of materials of petroleum origin (*ii*) the properties limit of some used materials. Therefore, production of innovative bionanocomposites derived from natural sources is currently one of the main points of interest in the academic and industrial areas of material research. Studies based on bio-nanocomposites using cellulose as reinforcing phase have been reported by many research groups in recent years [1, 2]. Cellulose is the most abundant polysaccharide on earth. It is a highly ordered polymer of cellobiose (D-glucopyranosyl-β-1,4-D-glucopyranose) chains aggregated by numerous strong intermolecular hydrogen bonds between hydroxyl groups of adjacent macromolecules. Cellulosic nanofibers present crystalline domains separated by less ordered ones

called amorphous regions. Crystalline and amorphous domains are found in native cellulose fibers in variable ratios, as a function of the plant species, with the growing conditions or the part of the plant.

In literature, cellulose nanofillers were used as reinforcing phase on polymers based nanocomposites [2, 3]. When small amounts of cellulose nanofillers are introduced into the matrix, some changes in Young's modulus, tensile strength, thermal stability, dielectric strength and electrical conductivity had been brought. The current study is in keeping with the general pattern aiming at the valorization of nanocellulose from the rachis of the date palm tree. Cellulose nanocrystals (CNC) and nanofibrils (NFC) are used as reinforcing phase for the Natural Rubber (NR) polymer. Natural rubber (NR) has a low glass transition temperature, T_g, soft elastomer characteristics at room temperature, and good elastic and adhesive properties [4]. The choice of the matrix was dictated by the fact that it is a natural polymer, often reinforced with nanoparticles and available as latex. Natural nanocomposites can be used in automotive industry, biomedical applications, packaging industry [5], humidity sensors [6] and microporous separators in batteries [7].

This work aims to study the effect of the addition of cellulose nanofillers on the mechanical and the dielectric properties of NR-based nanocomposites.

2. Experimental

2.1. Materials

2.1.1. Polymer matrix. Natural rubber (NR) was kindly supplied as NR latex by Michelin (Clermont-Ferrand, France) and used as matrix material. It contained spherical particles with an average diameter around 1 μm and its solid content was about 50 wt%. The density of dry NR, ρ_{NR}, was 1g.cm^{-3} and it contained more than 98% of cis-1, 4-polyisoprene [8]. Its glass transition temperature was around -61 °C.

2.1.2. Nanofibrillated cellulose and cellulose nanocrystals. (NFC) and (CNC) were extracted from the rachis of the date palm tree. Colloidal suspensions of NFC and CNC in water were prepared as described elsewhere [9, 10]. The rachis of date palm tree was mashed and extracted using soxhlet with a toluene/ethanol mixture (38/62 v/v) to remove pigments, lipids and waxes. The obtained cell walls were then dried at 80 °C for 2 hours. After wet grinding in a blender, the fibers underwent an alkaline treatment. Then, the fibers were bleached with sodium chlorite to remove lignin. The main difference between the preparation of NFC and CNC was the last step in which the bleached cellulose was disintegrated by pumping through a microfluidizer processor (Model M-110 EH-30) instead of submitting it to an acid hydrolysis treatment. The solid content of the suspensions was around 0.3 wt%. (NFC) had an average length of 700 nm ~ 1100 nm and an average width of 8 nm ~ 12.5 nm while (CNC) had an average length of 100 nm ~ 400 nm and an average width less than 10 nm [8]. In this study, a series of nine samples was used (Table1). The numbers indicate the nanoparticle content, in weight.

Table 1. Codification and composition of nanocomposite films based on NR.

Samples		Nanofiller content (%)
NR		0
NR-NFC1	NR-CNC1	1
NR-NFC2.5	NR-CNC2.5	2.5
NR-NFC7.5	NR-CNC7.5	7.5
NR-NFC15	NR-CNC15	15

2.2. Experimental methods

2.2.1. Dielectric measurements. Dielectric measurements were carried out using a Novocontrol Impedance Spectrometer based on an Alpha analyzer and a Quatro temperature controller in the frequency range 0.1 Hz – 1 MHz and in the temperature range from -100 °C to 200 °C in steps of 10 °C and at an oscillation voltage of 1 V. A film of each sample was placed between two brass plated electrodes (diameter 20 mm) of a parallel plate capacitor. The sample was mounted in a cryostat, and the temperature was controlled by a heated gas stream of nitrogen, evaporated from the liquid state. The temperature was controlled by a nitrogen jet (Quatro, Novocontrol), with an uncertainty of 0.1 °C during every frequency sweep.

According to the planar capacitor rule, the complex dielectric function is expressed as [11]:

$$\varepsilon^*(\omega) = \varepsilon'(\omega) - j\varepsilon''(\omega) \quad (1)$$

The accuracy of Alpha impedance measurement is 0.01%.

2.2.2. Tensile tests. The mechanical strength of various films was measured with a RSA3 (TA Instruments, USA) with a load cell of 100 N to identify any change in their physical properties upon the addition of NFC or CNC into the NR film. The specimens were prepared to be 5 mm in width and 40 mm in length. Samples were conditioned at room temperature for at least 48 h before testing and tested using a programmed elongation rate of 50 mm min^{-1}. Load, displacement and strain were recorded during the test by means of an acquisition system connected to a computer. True stress σ and true strain ε were given by the relationships [12]:

$$\varepsilon = \ln\left(\frac{L}{L_0}\right) \quad (2)$$

$$\sigma = \frac{F}{S} \quad (3)$$

Using the law of conservation of volume ($SL=S_0L_0$), the true stress is written:

$$\sigma = \frac{FL}{S_0 L_0} \quad (4)$$

where F, L_0, S_0, L and S were the applied force, the initial sample length, the initial sample section, the length and the sample section during the test, respectively.

2.2.3. Dynamic Mechanical Analysis. The viscoelastic properties of the polymers were determined via Dynamic Mechanical Analysis (DMA) using an apparatus DMA RSA3 from TA Instruments working in the tensile mode. Rectangular strips with dimensions around 40 x 5 x 1mm^3 from all nanocomposite films as well as the neat NR film were prepared. Measurements were carried out each two degrees from -100 °C to 250 °C at a frequency of 1 Hz. The properties determined under this oscillating loading conditions were storage modulus (E'), loss modulus (E'') and damping factor (tanδ). In DMA, E' is a measure of stored energy without phase difference between stress and strain and represents the elastic component of a viscoelastic material; E'' is a measure of the energy lost as heat and represents the viscous component of a viscoelastic material; δ represents the phase lag between the applied stress and the corresponding strain in a viscoelastic material, while tanδ is the ratio of loss modulus to storage modulus (E''/E') and is a measure of the energy dissipation or damping. tanδ reaches a

maximum as the polymer undergoes a transition from the glassy to the rubbery state at the glass transition temperature, T_g.

3. Results and discussion

3.1. Dielectric properties

Fig.1.a. and Fig.1.b. show the temperature dependence of the dielectric permittivity ε' and loss factor ε'', respectively, for the NR matrix. Dielectric measurements present three temperature regions of response assigned to:

(*i*) the primary relaxation associated with the glass transition and characterizing the α dipolar dynamic relaxation [13].

(*ii*) the water dipoles relaxation. Since NR has no hydrophilic groups, this observation suggests that water is connected to the hydroxyl groups (−OH) of the lipid present in NR [9].

(*iii*) the ionic conduction process appearing for high temperature and low-frequency ranges, which arises from the increase in the mobility of the electric charges in the polymer with temperature, with a large increase in both the real and imaginary parts of the dielectric function [14, 15].

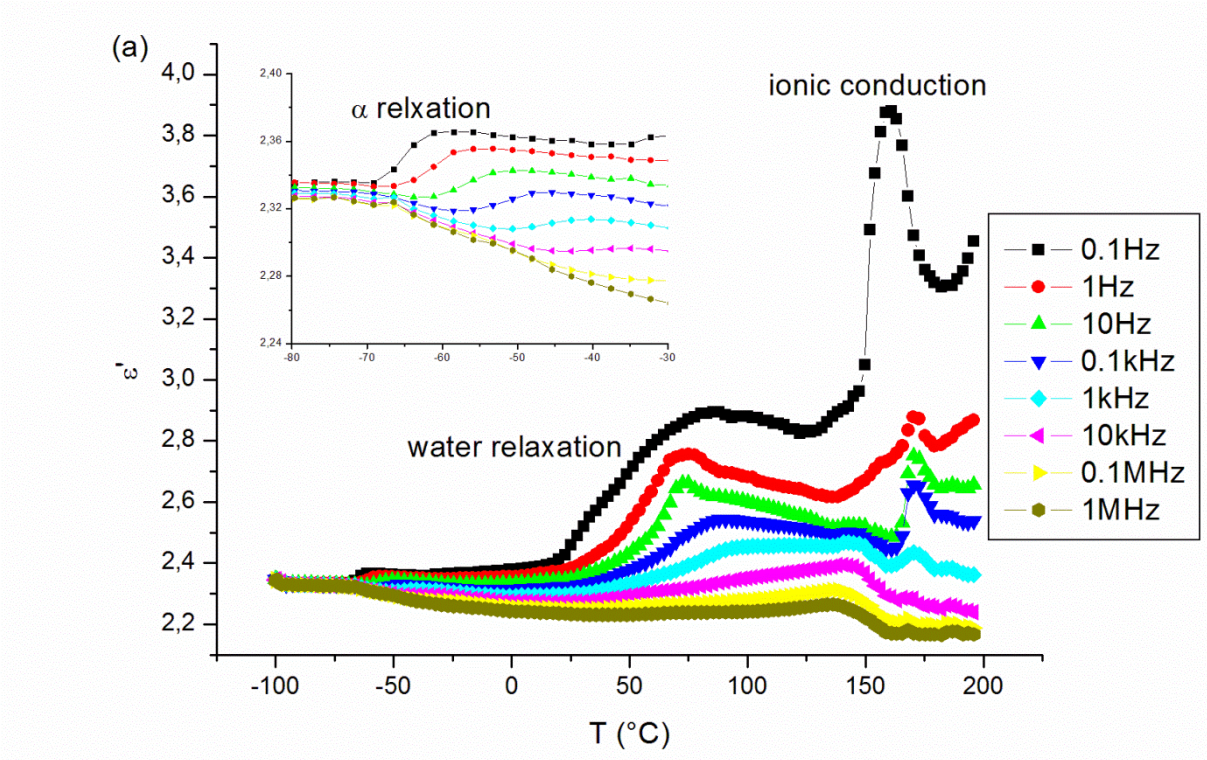

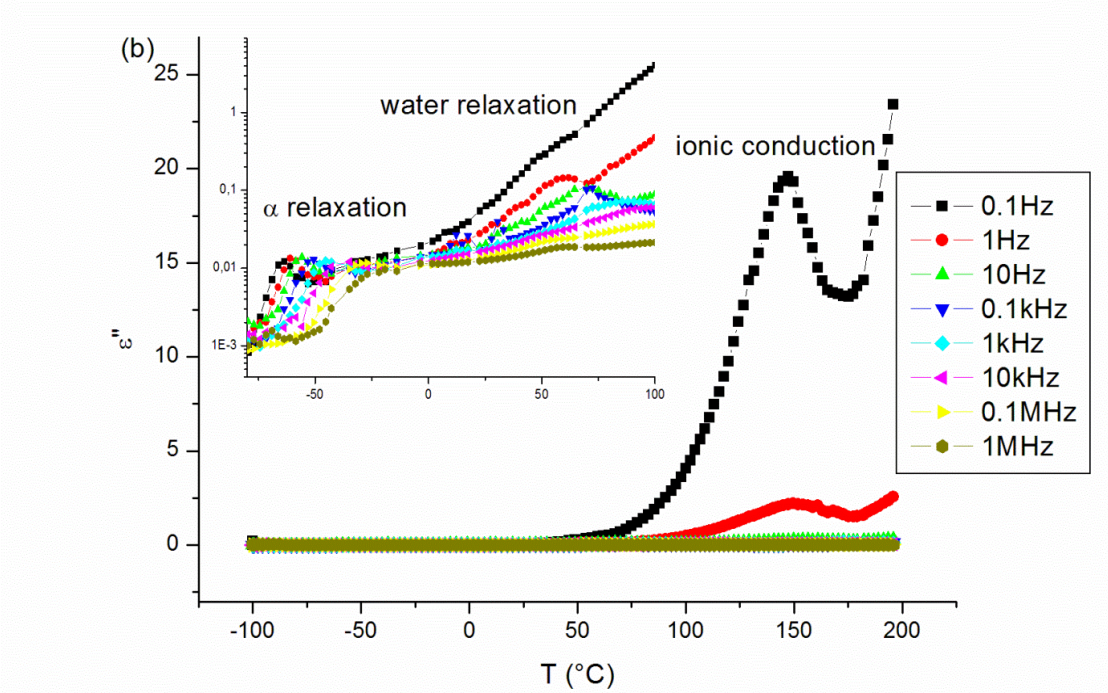

Fig. 1. Real and imaginary parts of the complex permittivity versus temperature, for the NR matrix.

In Fig. 2, the incorporation of cellulose nanofillers has an amplification effect of the dielectric losses. The polarity of cis-1,4-isoprene molecules is very low, so the loss data will be strongly influenced by dipolar impurities along the chains and in the bulk. The high value of the imaginary part of the permittivity of the nanocomposite material should be also due to the presence of water and impurities present on the cellulose nanofillers. The water dipoles relaxation is increasing when introducing hydrophilic cellulose. In addition, an interfacial polarization was detected. The interfacial polarization effect arises from the fact that free charges (catalysts, impurities, etc.), which were present at the stage of the processing, are immobilized in the material. These free carriers are then blocked at the interface between the cellulose nanofillers and NR matrix [16].

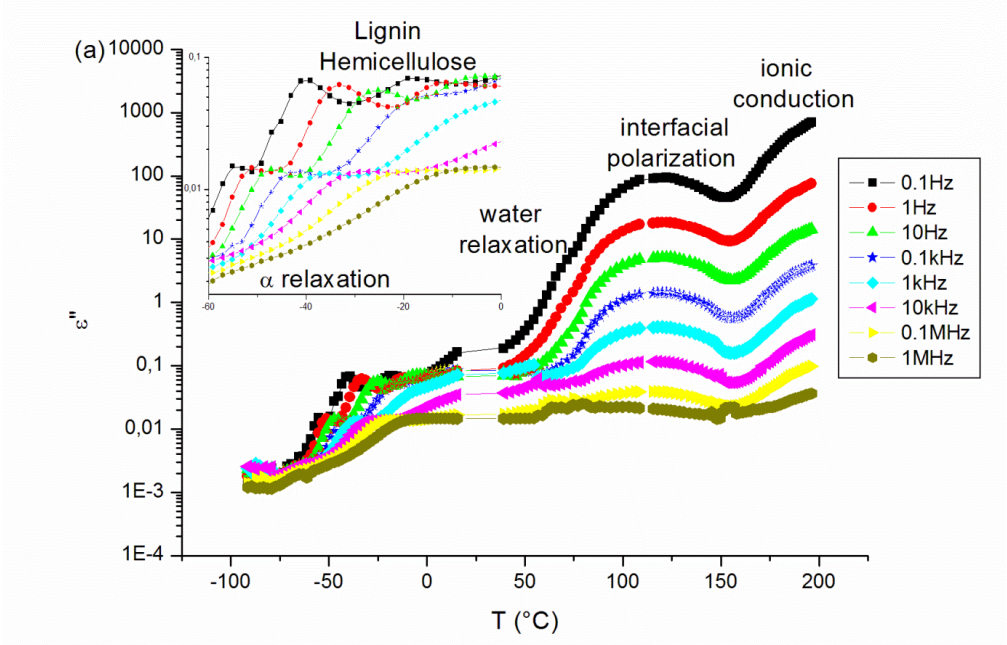

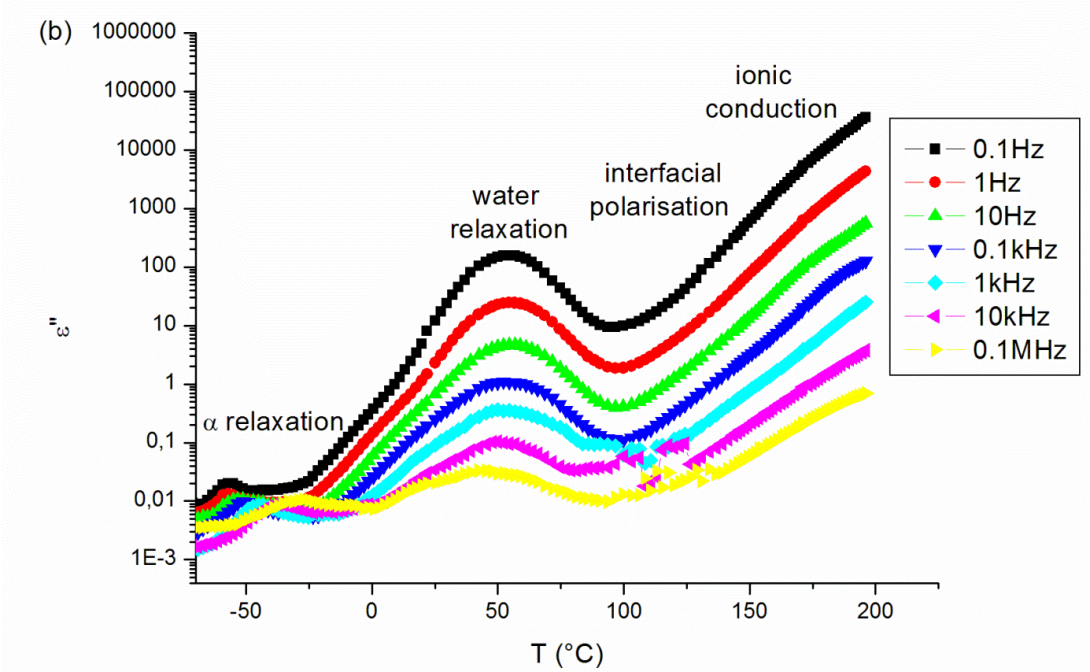

Fig. 2. Imaginary part of the complex permittivity, as a function of temperature, for (a) the NR-NFC7.5 and (b) NR-CNC7.5 nanocomposite.

In the dielectric study, isothermal runs give more information, and relaxation phenomena are investigated at the studied frequency range. However, relaxation peaks are often hidden with the large increase in permittivity values and loss at low-frequencies. The familiar difficulties of the ionic conduction phenomenon can be resolved using the first derivative of the real part of the dielectric permittivity [17]:

$$\varepsilon''_{der} = -\frac{\pi}{2}\frac{\partial \varepsilon'}{\partial \ln \omega} \qquad (5)$$

As the $\varepsilon'(\omega)$ values are in principle not affected by the Ohmic conductivity, and according to the Kramers-Kroning relationships, its derivative is proportional to the part of $\varepsilon''(\omega)$ resulting from dipolar processes [18]. Indeed, in the derivative formalism, the relaxation processes visible in the dielectric loss data appear as sharper peaks and without the conductivity contribution [19].
In Fig. 3, we compare the dielectric loss derivative data ε''_{der} at 150 °C for the NR, NR-NFC7.5 and NR-CNC7.5 films. For the NR matrix, we identify tow relaxation peaks attributed both to the relaxation of the lipid portion present in NR as a natural impurity [20, 21]. Lipid groups appeared on the NMR spectrum of NR performed in Ortiz-Serna work [20]. For nanocomposite samples, the lipid dipoles relaxations are hidden with the interfacial polarization.

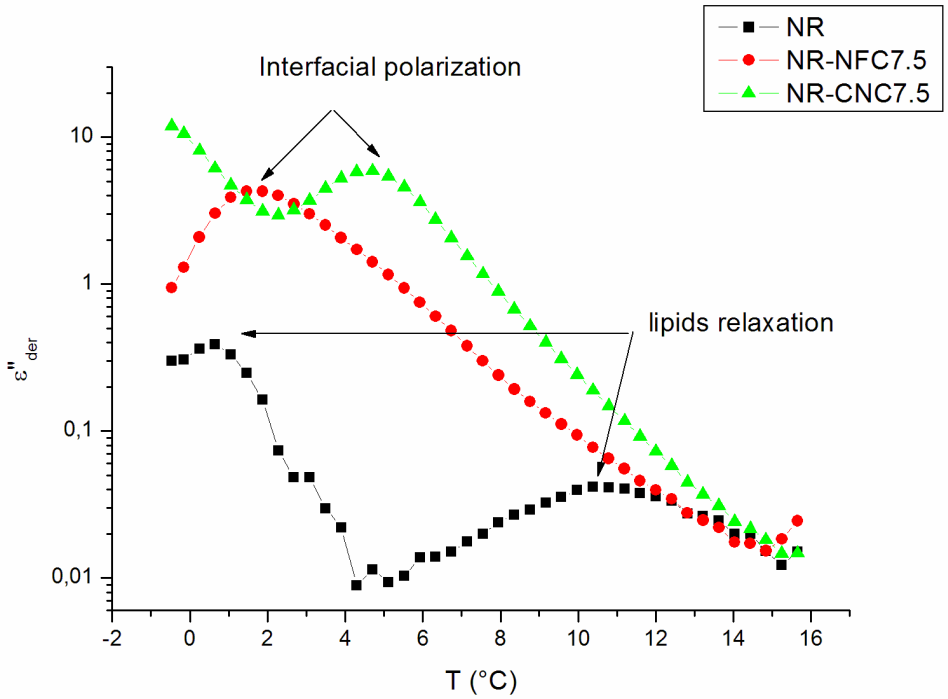

Fig. 3. The first derivative of the real part of the dielectric permittivity versus frequency at 150 °C.

To evaluate the effect of the reinforcement, the interfacial polarization (informing about the quality of the interface) is investigated. An analysis based on fitting using appropriate model functions is performed. The dielectric spectra (isothermal runs) were fitted by a sum of Havriliak-Negami (HN) model function terms of the form [22, 23]:

$$\varepsilon^*(\omega) = -i\left(\frac{\sigma_0}{\varepsilon_0\omega}\right)^N + \sum_{i=1}^{n}\left[\left(\varepsilon_{i\infty} + \frac{\Delta\varepsilon_i}{\left[1+(i\omega\tau_i)^{\alpha_i}\right]^{\beta_i}}\right)\right] \quad (6)$$

Where the term $-i\left(\frac{\sigma_0}{\varepsilon_0\omega}\right)^N$ is the contribution from polarization effects at the electrode, σ_0 is the DC conductivity, ε_0 is the permittivity of free space, and $\omega = 2\pi f$ is the radian frequency and N is a fractional exponent. Electrode polarization is ohmic when $N = 1$. The term $\sum_{i=1}^{n}\left[\left(\varepsilon_{i\infty} + \frac{\Delta\varepsilon_i}{\left[1+(i\omega\tau_i)^{\alpha_i}\right]^{\beta_i}}\right)\right]$ is the contribution of the dipolar orientations which are summed for the number of relaxation processes being fit simultaneously. $\varepsilon_{i\infty}$ is the real permittivity at $\omega = \infty$ of the ith relaxation process; $\Delta\varepsilon_i = \varepsilon_{si} - \varepsilon_{\infty i}$, is the dielectric relaxation strength where ε_{si} is the real permittivity at $\omega = 0$; τ_i is the relaxation time of the i_{th} relaxation process; α_i and β_i are the fractional shape parameters that respectively define the breadth and symmetry of the i_{th} relaxation process.
The polarization strength $\Delta\varepsilon$ is defined for static electric fields as [24–27]:

$$\Delta\varepsilon = \frac{4\pi F N_A \rho g \mu^2}{3\varepsilon_0 M_w k_B T} \quad (7)$$

Here $F\left(=\frac{\varepsilon_s(\varepsilon_\infty+2)^2}{3(2\varepsilon_s+\varepsilon_\infty}\right)$ is the Onsager factor for local field effects, N_A is Avogadro's number, M_w is the molecular weight, ρ is the density, k_B is Boltzmann's constant, g is the Kirkwood–Frohlich correlation factor and μ^2 is the mean squared dipole moment in the gas phase.

According to the table 2, the high increase in the polarization strength $\Delta\varepsilon$ with temperature is explained with the increase in the induced dipoles mobility. In addition, at a fixed temperature, $\Delta\varepsilon$ increases with filling up to a threshold value and then decreases. In fact, total interface area is increased with filling. The number of trapped dipoles at the interface is increased, increasing thus $\Delta\varepsilon$. Above a critical filler contain, the interface becomes sufficiently charged, and the interactions between the dipoles become more important. $\Delta\varepsilon$ then decreases indicating a rigid interface. In the other hand, and as it can be seen from table 2, one can predict that the nanocomposite reinforced with CNC has higher values of $\Delta\varepsilon$ than which reinforced with NFC. In fact, the number of trapped charges at the interface NR/CNC is more important than NR/NFC. Strong interactions between induced dipoles located at the interface NR/CNC indicate stiff interfaces. Therefore, this result indicates that the interfacial adhesion should be higher for NR/NFC than NR/CNC. It could be ascribed to the presence of residual lignin and hemicelluloses at the surface of NFC [18] acting as a compatibilizer between the filler and the matrix.

Table 2. The interfacial polarization strength $\Delta\varepsilon$ for different nanocomposites. The correlation coefficient, in all the cases, is larger than 0.997.

T (°C)	NR-NFC1	NR-NFC2.5	NR-NFC7.5	NR-NFC15
110	2.99	4.71	14.37	0.12
150	2.34	50.56	65.82	39.55
190	-	56.19	112.75	97.70
	NR-CNC1	NR-CNC2.5	NR-CNC7.5	NR-CNC15
110	12.33	40.65	30.12	12.84
150	36.52	85.13	79.33	54.32
190	80.64	190.25	155.95	101.60

3.2. Tensile properties

Tensile tests were run in order to evaluate the interactions between the fillers and the polymer matrix. Extracted parameters derived from Stress-Strain tensile tests are reported in Table 3.

Table 3. Young modulus (E), strain at break (ε_R) and strength (σ_R).obtained from the tensile tests [8].

Samples	E (MPa)	σ_R (MPa)	ε_R (%)
NR	0.5	0.56	575
NR-NFC1	1.27	0.7	209
NR-NFC2.5	10.52	0.8	14.6
NR-NFC7.5	121.2	4.15	8.18
NR-NFC15	233	6.26	3.95
NR-CNC1	1.7	0.86	408
NR-CNC2.5	2.8	1.17	358
NR-CNC7.5	59.2	5.7	170
NR-CNC15	187	12.15	14

For both sets of nanocomposites, the elongation at break decreases and both the tensile modulus and the strength increase drastically when increasing the nanoparticles content. The tensile modulus is systematically higher for a given composition for NFC reinforced nanocomposites compared to CNCs,

whereas both the strength and the elongation at break are lower. These results seem in discordance with those of Ismail et al. [28] and Zhong Xian Ooi et al. [29] whose studied the reinforcement of natural rubber by carbon particles. The authors reported that a smaller particle size normally gives better interaction with the natural rubber matrix. The carbon black has the smallest particle size, thus the carbon black–filled NR vulcanizates showed the highest tensile strength and the lower strain at break followed by oil palm ash (OPA) and silica–filled vulcanizates. The presence of residual lignin and hemicelluloses at the surface of NFC could probably explain this discordance. Entangled NFC provide a higher stiffness than CNCs but induce brittleness of the material. Similar results were reported for chemically modified cellulose CNCs and MFC extracted from sisal reinforced polycaprolactone [30]. The presence of these impurities explains the higher compatibility of NFC with the hydrophobic NR matrix, and the ensuing higher filler/matrix adhesion. This higher NFC reinforcing effect was already evidenced from the dielectric study.

3.3. Dynamic Mechanical properties

The thermo–mechanical behavior of NR nanocomposites was studied by (DMA) analysis. Compared to tensile tests, this technique allows following the mechanical properties in a large temperature range. Fig. 4(a) shows the evolutions of the storage tensile modulus, log (E'), and the loss angle tanδ versus temperature at 1 Hz for NR, NR-NF2.5 and NR-CNC2.5. Modulus values have been normalized at low temperature at 1 GPa to allow a better comparison. The curve corresponding to the unfilled NR matrix is typical for high molecular weight amorphous thermoplastic polymer. The sharp decreases over 3 decades observed around -60 °C corresponds to the main relaxation phenomenon. It occurs in the same temperature range as T_g and it is therefore associated with the inelastic manifestation of the glass transition. The global evolution for nanocomposite films is similar to the one of the neat matrix. At low temperature, i.e., below T_g, the reinforcing effect of cellulosic nanofillers was low justifying the normalization of the modulus. Above T_g, a much more significant reinforcing effect of the nanofillers was observed. The NR-NFC2.5 nanocomposite has a higher E' than the NR-CNC2.5 nanocomposite, suggesting that the interactions between the NR matrix and the NFC fibers were stronger. As explained in the tensile test part, this could be ascribed to the presence of residual lignin and hemicelluloses at the surface of NFC [31] acting as a compatibilizer between the nanofiller and the matrix.

This result is confirmed in tanδ curves (Fig 4). As the dielectric study, only for the NR-NFC2.5 nanocomposite, the main relaxation process splits into two well–defined peaks. This splitting of the relaxation process could be ascribed to strong interactions between NFC and NR matrix because of the presence of residual lignin and hemicelluloses at the surface of NFC as already suggested. These interactions could lead to the formation of an interfacial layer surrounding the filler and which mobility is restricted compared to the bulk matrix. In addition, the NR matrix has the highest tanδ value indicating that there is a large degree of mobility, thus good damping behavior [46]. Reinforcement of NR with NFC or CNC nanofillers decreased the damping behavior of the nanocomposites as cellulose acted as a barrier to the free movement of the molecular chain. In addition, cellulose nanocomposites show lowest tanδ peak value and lowering of peak value also indicative of good interfacial adhesion [32].

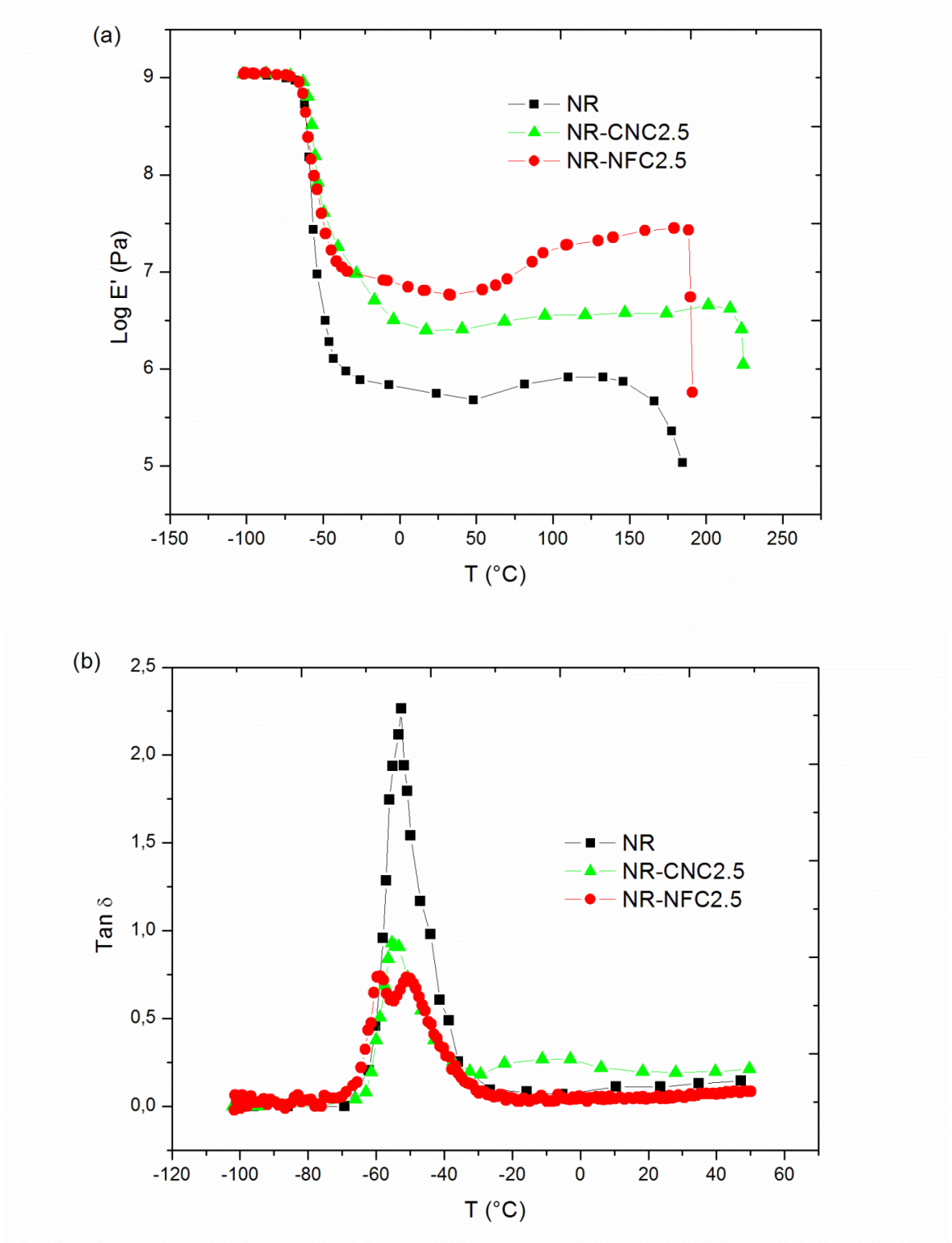

Fig. 4. Logarithm of the storage modulus (*E'*) and tan*δ* curves vs. temperature for NR matrix, NR-NFC2.5 and NR-CNC2.5 nanocomposites.

These results clearly highlight that the interfacial adhesion is higher for NR/NFC nanocomposite compared to NR/CNC. This difference is manifested by the presence of a second relaxation attributed to constrained interfacial NR chains interacting with lignin (Scheme 1).

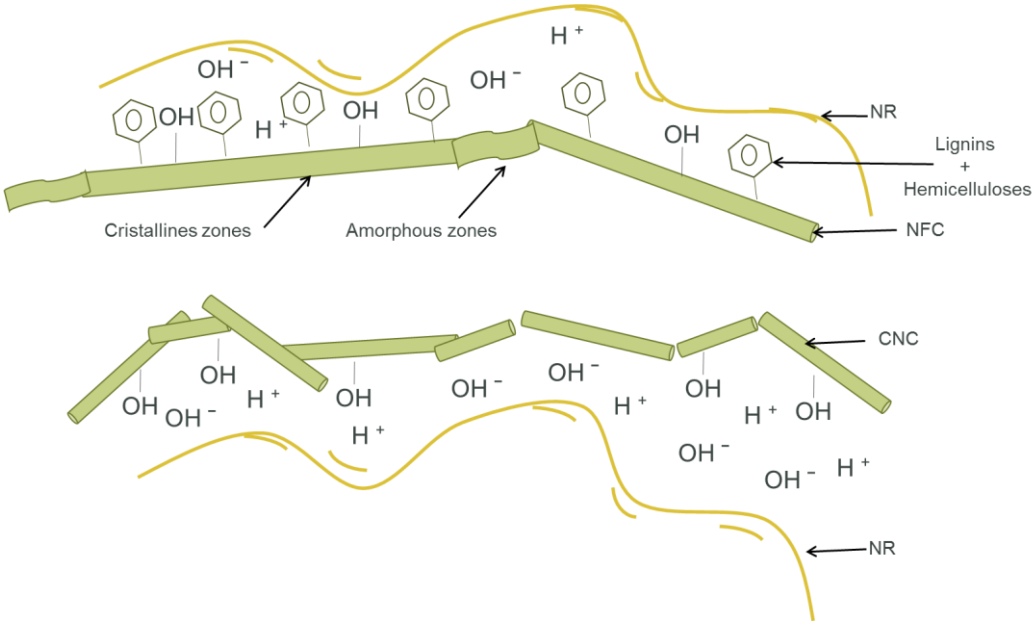

Scheme 1. Schematic illustration of the NR–NFC and NR–CNC interfaces.

4. Conclusion

This work emphasizes the cellulose nanofillers effect on the physical properties of NR based bio-nanocomposites. It attempts to give an overview of ongoing studies on dielectric, mechanical and dynamic mechanical properties of NR/NFC and NR/CNC nanocomposites. Being able to control the interface makes it possible to achieve the greatest improvement in the dielectric properties without strongly affecting the mechanical properties. By studying two different types of fibers, it was found that residual lignin and hemicelluloses surrounding NFC increase the tensile modulus and decrease the deformation at break. These impurities thus improve the interfacial adhesion between fibers and matrix. Moreover, the storage modulus E' is higher and the damping factor tanδ is lower for NR-NFC2 compared to NR-CNC2.5. This result suggests that the interactions between the NR matrix and NFC fibers were stronger. In addition, fiber size influences the dielectric properties of the resulting nanocomposites. Cellulose nanocrystals are smaller than nanofibrillated cellulose and CNCs generate more interfaces. Strong interactions between induced dipoles located at the NR/CNC interface indicate stiff interfaces. Therefore, the interfacial adhesion should be higher for NFC/NR than for NR/CNC.

References

[1] Boufi S and Chaker A 2016 Easy production of cellulose nanofibrils from corn stalk by a conventional high speed blender *Ind. Crop. Prod.* **93** 39-47.

[2] Ladhar A, Arous M, Kaddami H, Raihane M, Kallel A, Graça M P F and Costa L C 2014 Molecular dynamics of nanocomposites natural rubber/cellulose nanowhiskers investigated by impedance spectroscopy *J. Mol. Liq.* **196** 187-191.

[3] Benhamou K, Kaddami H, Magnin A, Dufresne A and Ahmad A 2015 Bio-based polyurethane reinforced with cellulose nanofibers: A comprehensive investigation on the effect of interface *Carbohyd. Polym.* **122** 202–211.

[4] Kamisan A S, Kudin T I T, Ali A M M and Yahya M Z A 2009 Gel polymer electrolyte based on methyl-grafted natural rubber for proton batteries *Mater. Res. Innov.* **13** 263–265.

[5] Chiappone , Nair J R, Gerbaldi C, Jabbour L, Bongiovanni R, Zeno E, Beneventi D and Penazzi N 2011 Microfibrillated cellulose as reinforcement for Li-ion battery polymer electrolytes with excellent mechanical stability, *J. Power Sources* **196** 10280–10288.

[6] Ummartyotin S, Manuspiya H, 2015 A critical review on cellulose: from fundamental to an

approach on sensor technology, *Renew. Sustain. Energy Rev.* **41** 402–412.
[7] Xu Q, Kong Q, Liu Z, Wang X, Liu R, Zhang J, Yue L, Duan Y and Cui G 2014 Cellulose/ polysulfonamide composite membrane as a high performance lithium-ion battery separator *ACS Sustain. Chem. Eng.* **2** 194–199.
[8] Bendahou A, Kaddami H and Dufresne A (2010) Investigation on the effect of cellulosic nanoparticles' morphology on the properties of natural rubber based nanocomposites *Eur. Polym. J.* **46** 609–620.
[9] Dufresne A 2006 Comparing the mechanical properties of high performances polymer nanocomposites from renewable sources *J. Nanosci. Nanotechnol.* **6** 322–330.
[10] Dufresne A 2008 Polysaccharide nanocrystals reinforced nanocomposites *Can. J. Chem.* **86** 484–494.
[11] Arous M, Ben Amor I, Kallel A, Fakhfakh Z and Perrier G 2007 Crystallinity and dielectric relaxations in semi-crystalline poly(ether ether ketone) *J. Phys. Chem. Solids* **68** 1405–1414.
[12] Mariano M, El Kissi N and Dufresne A 2016 Cellulose nanocrystal reinforced oxidized natural rubber nanocomposites *Carbohydr. Polym.* **137** 174–183.
[13] Ladhar A, Arous M, Kaddami H, Raihane M, Lahcini M, Kallel A, Graça M P F and Costa L C 2013 Dielectric relaxation studies on nanocomposites of rubber with nanofibrillated cellulose *J. Non-Cryst. Solids* **378** 39–44.
[14] Ladhar A, Arous M, Kaddami H, Raihane M, Kallel A, Graça M P F, Costa L C 2015 Ionic hopping conductivity in potential batteries separator based on natural rubber–nanocellulose green nanocomposites *J. Mol. Liq.* **211** 792–802.
[15] Ladhar A, Arous M, Kaddami H, Raihane M, Kallel A, Graça M P F, Costa L C 2015 AC and DC electrical conductivity in natural rubber/nanofibrillated cellulose nanocomposites *J. Mol. Liq.* **209** 272–279
[16] Tsonos C, Apekis L, Zois C, Tsonos G 2004 Microphase separation in ion– containing polyurethanes studied by dielectric measurements *Acta Mater.* **52** 1319–1326.
[17] Kremer F, Schönhals A 2003 Broadband Dielectric Spectroscopy, Springer-Verlag, Berlin.
[18] Wübbenhorst M and Van Turnhout J 2002 Analysis of complex dielectric spectra. I. One-dimensional derivative techniques and three-dimensional modelling *J. Non-Cryst. Solids* **305** 40–49.
[19] Wübbenhorst M, Van Koten E, Jansen J, Mijs W and Van Turnhout J 1997 Dielectric relaxation spectroscopy of amorphous and liquid crystalline side chain polycarbonates *Macromol. Rapid Commun.* **18** 139.
[20] Ortiz-Serna P, Dıiaz-Calleja R, Sanchis M J, Floudas G, Nunes R C, Martins A F and L L Visconte 2010 Dynamics of Natural Rubber as a Function of Frequency, Temperature, and Pressure. A Dielectric Spectroscopy Investigation *Macromolecules* **43** 5094–5102.
[21] Ortiz-Serna P, Carsí M, Redondo-Foj B and Sanchis M J 2014 Electrical conductivity of natural rubber–cellulose II nanocomposites *J. Non-Cryst. Solids* **405** 180–187.
[22] Havriliak S, Negami S 1966 A complex plane analysis of α-dispersions in some polymer systems *J. Polym. Sci. C* **14** 99–117.
[23] Havriliak S and Negami S 1967 A complex plane representation of dielectric and mechanical relaxation processes in some polymers *Polymer* **8** 161–210.
[24] Langevin P 1905 Magnétisme et théorie des électrons *Ann. Chim. Phys.* **5** 70–127.
[25] Debye P 1929 Polar Molecules, The Chemical Catalogue Company, New York.
[26] Onsager L 1936 Electric Moments of Molecules in Liquids *J. Am. Chem. Soc.* **58** 1486–1493.
[27] Frohlich H 1958 Theory of Dielectrics, Oxford University Press, Oxford.
[28] Ismail H, Rozman, H D, Jaffri R M and MohdIshak Z A 1997 Oil palm wood flour reinforced epoxidized natural rubber composites: the effect of filler content and size *Eur. Polym. J.* **33** 1627–1632.
[29] Ooi Z X, Hanafi I and Abu Bakar A 2013 Optimisation of oil palm ash as reinforcement in natural rubber vulcanisation: A comparison between silica and carbon black fillers. *Polymer*

Testing **32** 625–630.
[30] Marchessault R H, Morehead F F and Walter NM 1959 Liquid crystal systems from fibrillar polysaccharides *Nature* **184** 632–633.
[31] Dufresne A, Cavaillé J Y and Vignon M R 1997 Mechanical behavior of sheets prepared from sugar beet cellulose microfibrils *J. Appl.Polym. Sci.* **64** 1185–1194.
[32] Jawaid M., Abdul Khalil H P S and Alattas O S 2012 Woven hybrid biocomposites: Dynamic mechanical and thermal properties *Composites: Part A* **43** 288–293.